

I. SUPPLEMENTAL MATERIAL

Here plots for all DDFT calculations can be found.

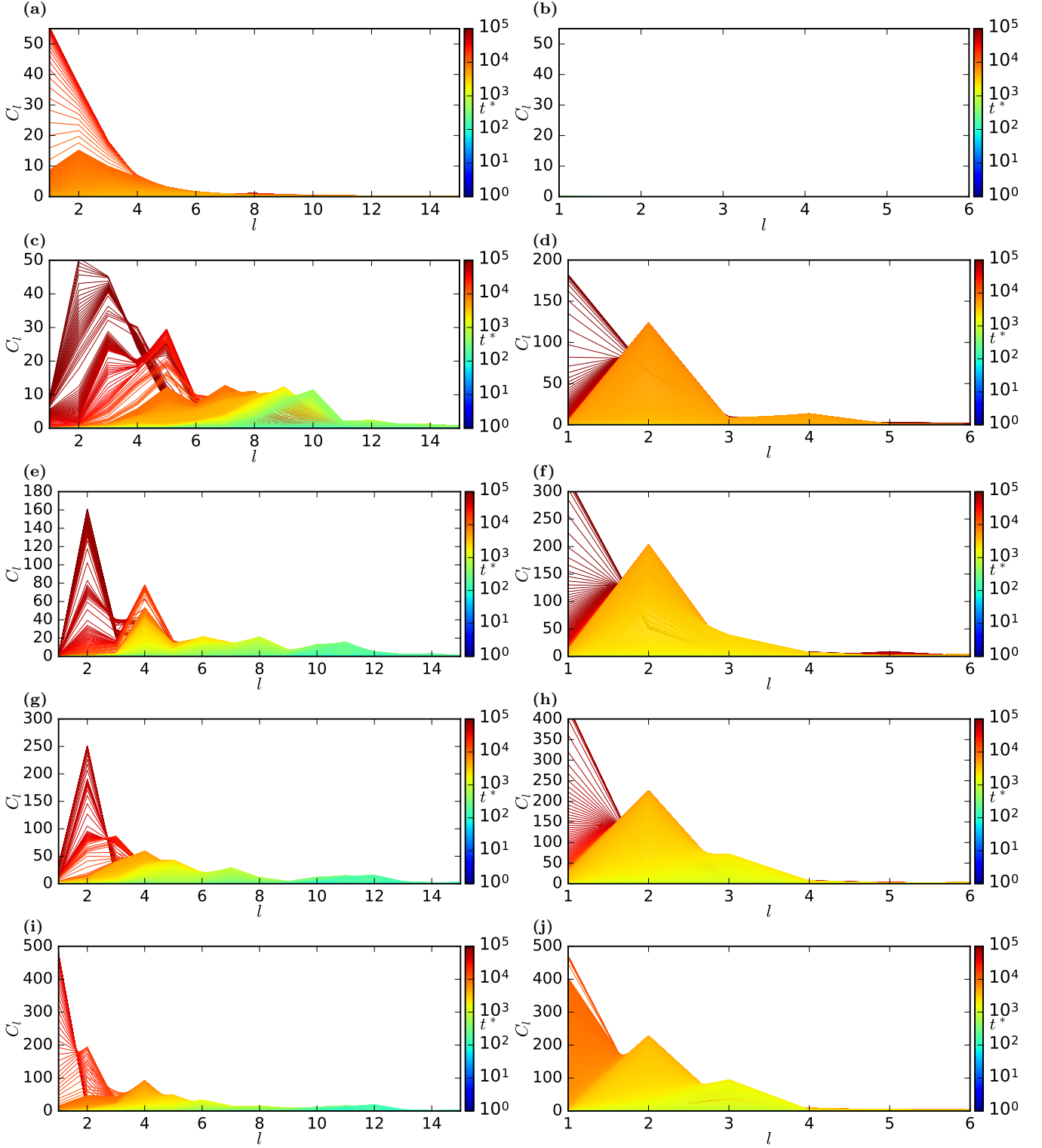


Figure 1. Angular power spectral density. Time t^* is color coded. First column: Large sphere $R = 10R_{11}$, second column: Small sphere $R = 2.5R_{11}$. First row: $x = 0.1$, second row: $x = 0.2$, third row: $x = 0.3$, fourth row $x = 0.4$, fifth row: $x = 0.5$.

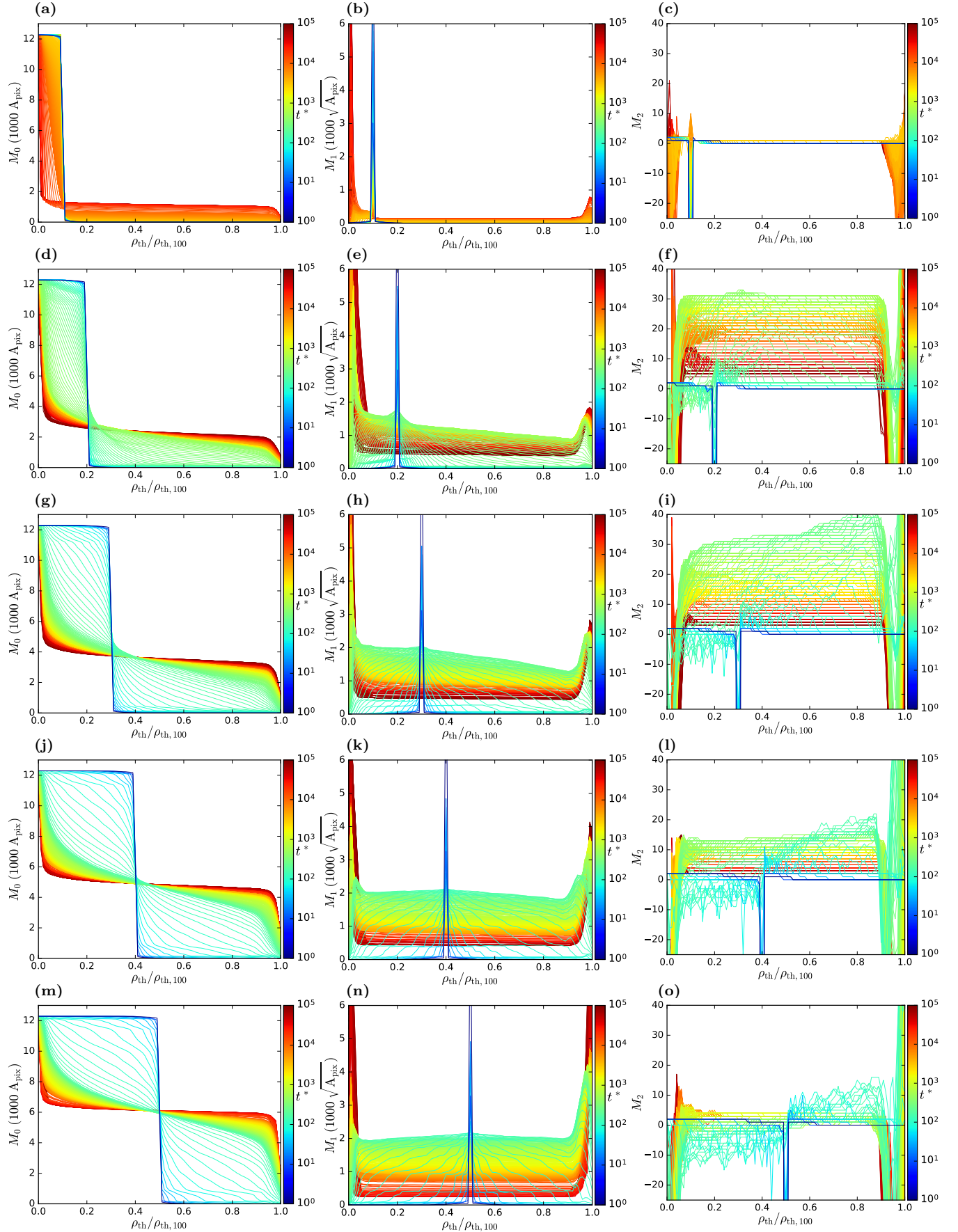


Figure 2. Minkowski functionals dependence on the threshold density $\rho_{\text{th}}/\rho_{\text{th},100}$ for the large sphere $R = 10R_{11}$. Time t^* is color coded. First column: Area functional M_0 , second column: perimeter functional M_1 , third column: euler functional M_2 . First row: $x = 0.1$, second row: $x = 0.2$, third row: $x = 0.3$, fourth row $x = 0.4$, fifth row: $x = 0.5$.

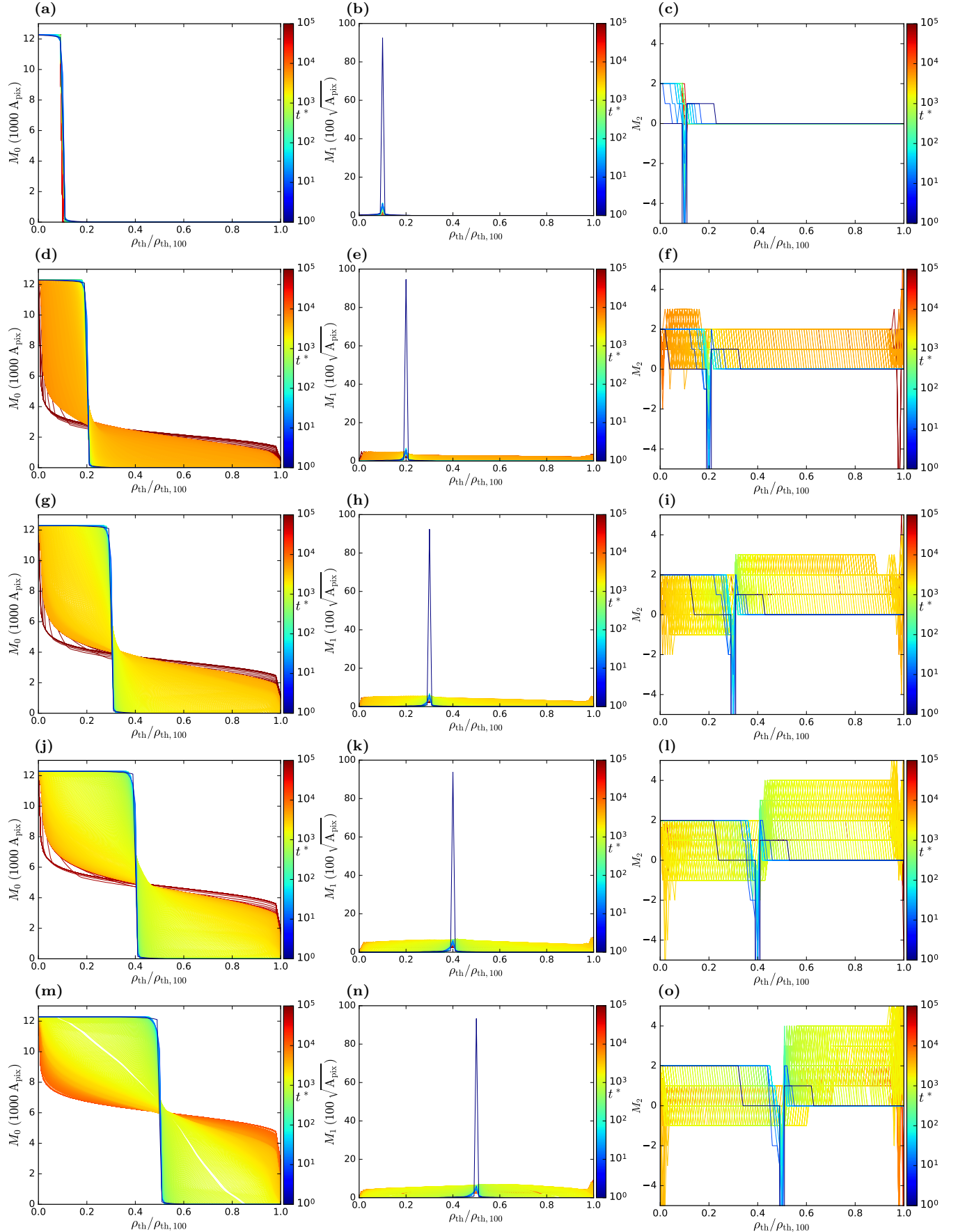


Figure 3. Minkowski functionals dependence on the threshold density $\rho_{\text{th}}/\rho_{\text{th},100}$ for the small sphere $R = 2.5R_{11}$. Time t^* is color coded. First column: Area functional M_0 , second column: perimeter functional M_1 , third column: euler functional M_2 . First row: $x = 0.1$, second row: $x = 0.2$, third row: $x = 0.3$, fourth row $x = 0.4$, fifth row: $x = 0.5$.

For early times of spinodal decomposition the time dependent functionals (Fig. 4 and Fig. 5) vary for different threshold density values. However, for later times the functionals become constant functions of ρ_{th} due to the emergence of well defined demixed domains. The functionals have their greatest variations at relative threshold values in the vicinity of the mixture parameter $\rho_{\text{th}}/\rho_{\text{th},100} \simeq x$. The variation of the functionals at $\rho_{\text{th}}/\rho_{\text{th},100} \simeq x$ decreases as time evolves due to the decrease of interfaces in the stage of domain coalescence. After the crossover time t_c^* between the spinodal decomposition and domain growth phase the functionals become constant functions. The area functionals M_0 for large times approach the constant value of the complete surface V_0 weighted with the mixing parameter x : $V(t \rightarrow \infty) = V_0x$. Correspondingly the perimeter functionals M_1 converge towards the value of the boundary length of the corresponding spherical cap. The Euler functional M_2 converges to the constant number of already demixed domains. For the extreme values of T one can observe peaks in M_1 and M_2 that originate from an artefact of the numerical implementation: the calculation of functional derivatives is done via convolutions of the spherical harmonical decomposition leading to overshoots at sharp edges of density variations at pixel boundaries. Since the analysis in the main paper only depends on intermediate values of ρ_{th} this does not pose a problem.

The number of domains can readily be obtained as the value of the Euler functional M_2 (Fig. 8). It counts the number of connected domains and subtracts the number of holes in the domains. Since for non-extreme threshold values (near the boundaries, e.g., $\rho_{\text{th}}/\rho_{\text{th},100} = 0$ and $\rho_{\text{th}}/\rho_{\text{th},100} = 1$) there are no holes in the domains, and the domains are disjoint, M_2 is exactly the number of already demixed domains.

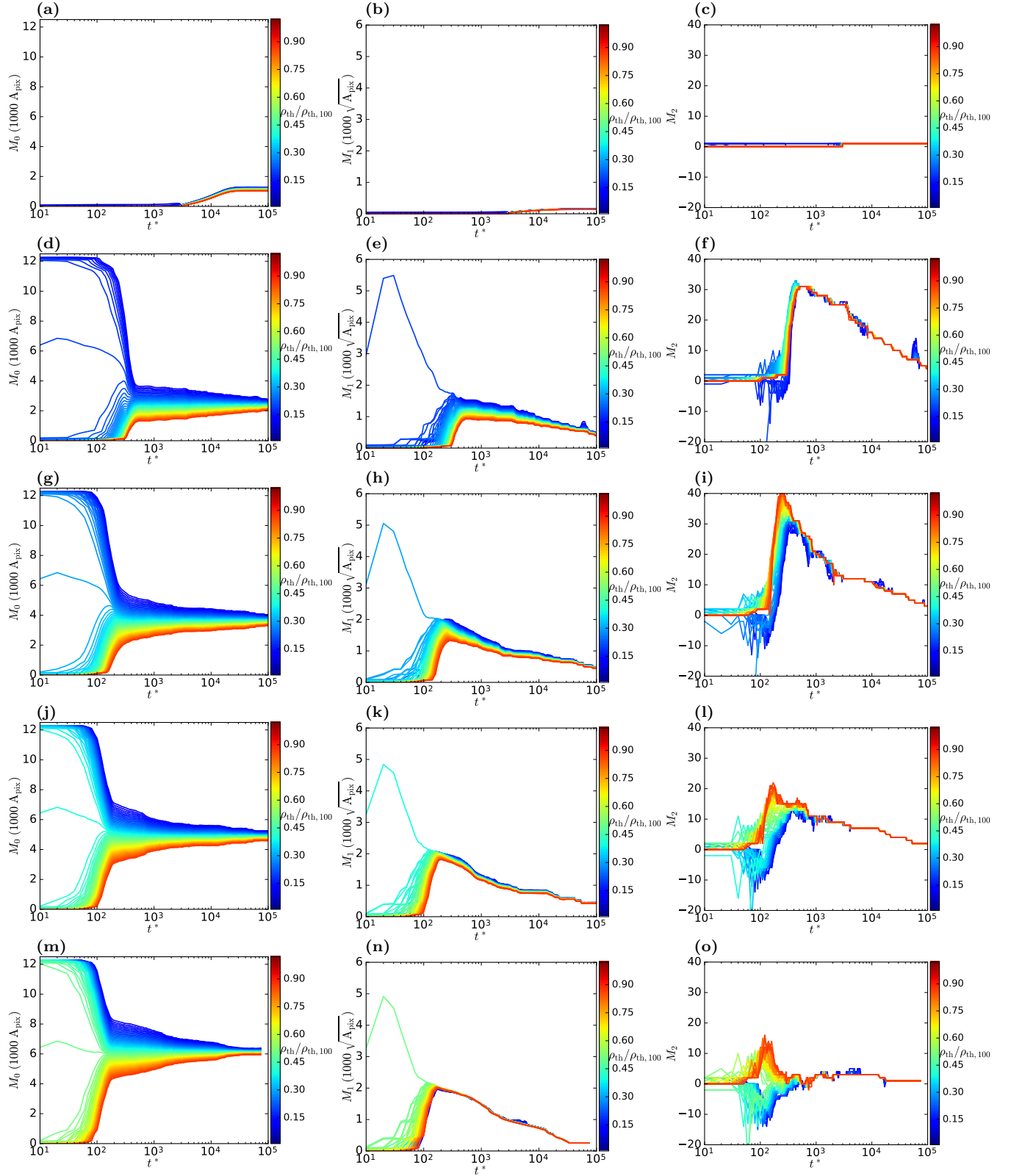


Figure 4. Minkowski functionals, dependence on time t^* , for the large sphere $R = 10R_{11}$. Threshold values $\rho_{\text{th}} / \rho_{\text{th},100}$ are color coded. First column: Area functional M_0 , second column: perimeter functional M_1 , third column: euler functional M_2 . First row: $x = 0.1$, second row: $x = 0.2$, third row: $x = 0.3$, fourth row $x = 0.4$, fifth row: $x = 0.5$.

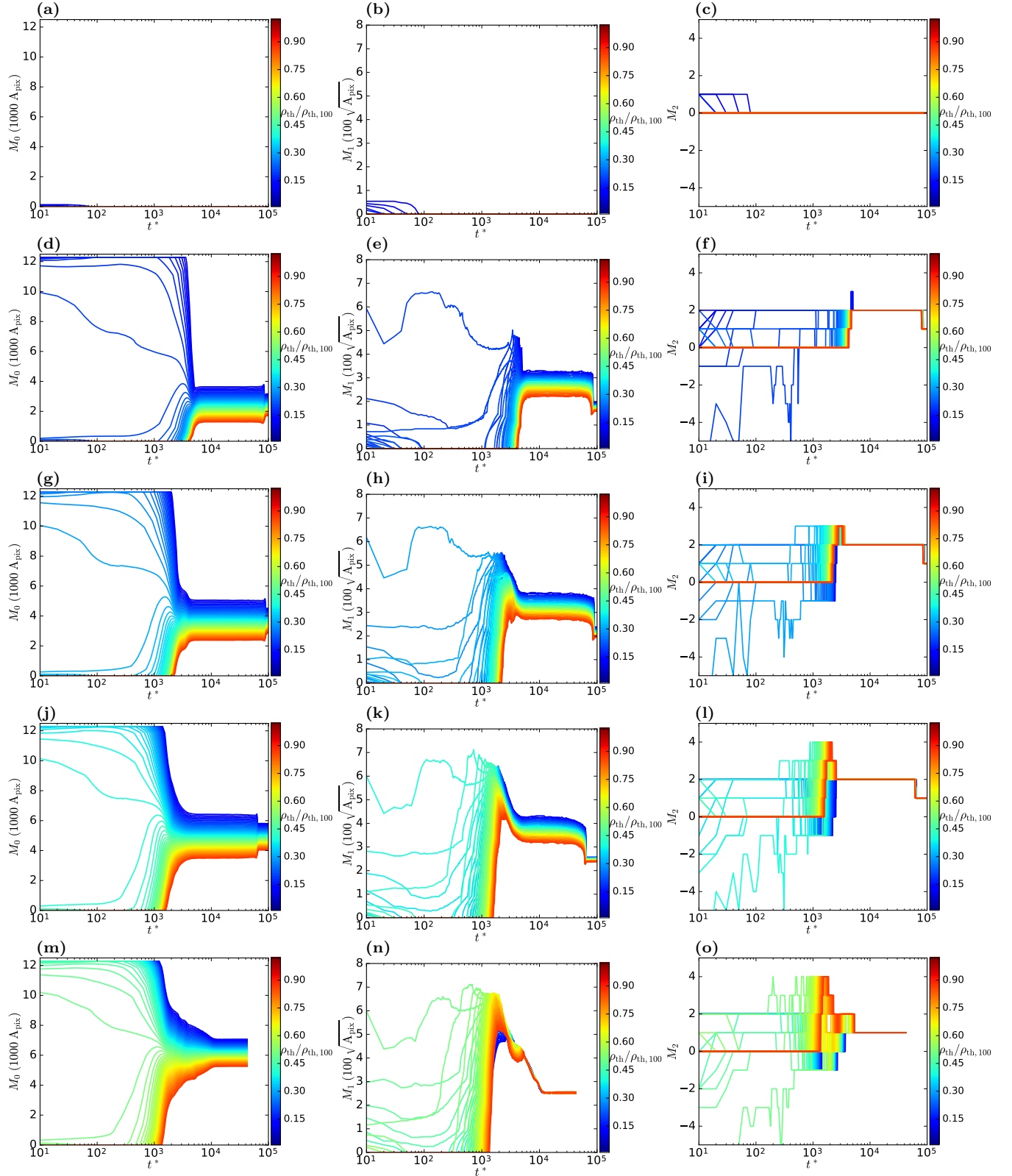


Figure 5. Minkowski functionals, dependence on time t^* , for the small sphere $R = 2.5R_{11}$. Threshold values $\rho_{\text{th}}/\rho_{\text{th},100}$ are color coded. First column: Area functional M_0 , second column: perimeter functional M_1 , third column: euler functional M_2 . First row: $x = 0.1$, second row: $x = 0.2$, third row: $x = 0.3$, fourth row $x = 0.4$, fifth row: $x = 0.5$.

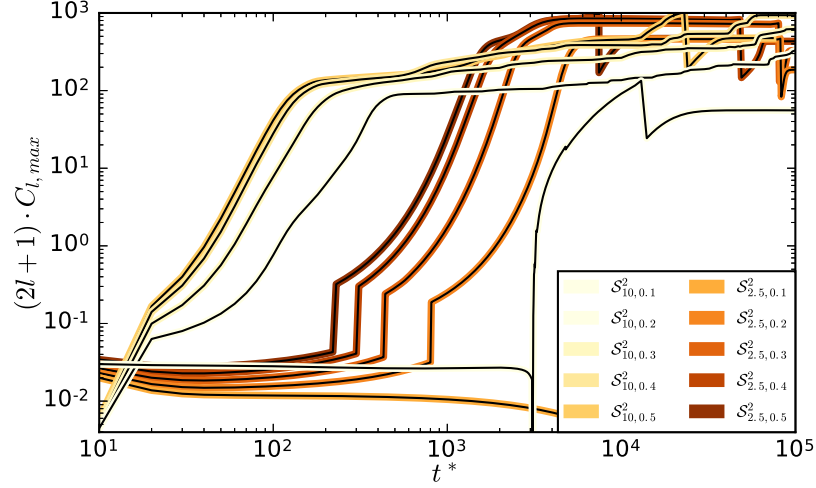


Figure 6. Power spectrum analysis: Power $(2l+1)C_{l,\max}$ of the maximum of the angular power spectrum $C_{l,\max} = \max_{1 < l < N}(C_l)$.

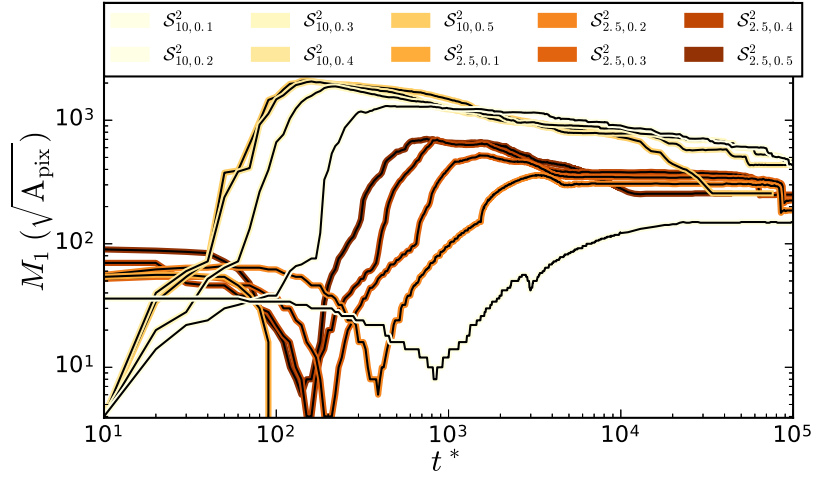


Figure 7. Circumference Minkowski functionals M_1 for threshold values $T/T_{100} \simeq x$. Exact threshold values are $\rho_{\text{th}}/\rho_{\text{th},100} \in [0.134, 0.212, 0.316, 0.416, 0.5154]$.

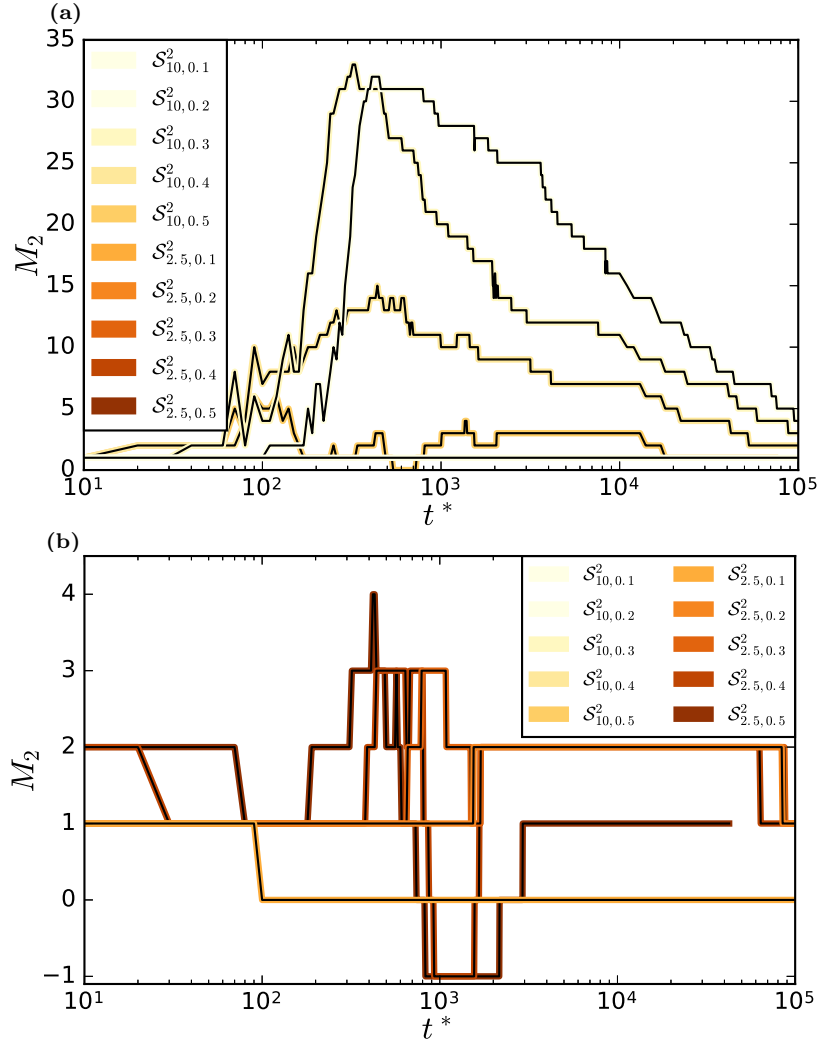


Figure 8. Euler characteristic Minkowski functional M_2 for threshold values $T/T_{100} \simeq x$. Exact threshold values are $\rho_{\text{th}}/\rho_{\text{th},100} \in [0.134, 0.212, 0.316, 0.416, 0.5154]$. (a) Large sphere $R = 10R_{11}$, (b) Small sphere $R = 2.5R_{11}$.